ISSN 0026-8933, Molecular Biology, 2006, Vol. 40, No. 3, pp. 433–439. © Pleiades Publishing, Inc., 2006.
Original Russian Text © I.A. Besschetnova, G.E. Pozmogova, A.N. Chuvilin, A.K. Shchyolkina, O.F. Borisova, 2006, published in Molekulyarnaya Biologiya, 2006, Vol. 40, No. 3, pp. 489–496.

STRUCTURAL–FUNCTIONAL ANALYSIS OF BIOPOLYMERS AND THEIR COMPLEXES

UDC 557.113.6

Complexes of Telomeric Oligonucleotide d(TTAGGG)$_4$ with the New Recombinant Protein Vector PGEk Carrying Nucleic Acids into Proliferating Cells

I. A. Besschetnova[a], G. E. Pozmogova[b], A. N. Chuvilin[c], A. K. Shchyolkina[a], and O. F. Borisova[a]

[a] *Engelhardt Institute of Molecular Biology, Russian Academy of Sciences, Moscow, 119991 Russia; e-mail: borisova@eimb.ru*

[b] *Bioengineering Center, Russian Academy of Sciences, Moscow, 119312 Russia*

[c] *Institute of Physico-Chemical Medicine, Ministry of Health and Social Development of the Russian Federation, Moscow, 119992 Russia*

Received December 15, 2005

Abstract—A study was made of the complexation of the protein vector PGEk, which transfers nucleic acids into the nuclei of cancer cells, with phosphodiester d(TTAGGG)$_4$ (TMO) and phosphorothioate Sd(TTAGGG)$_4$ (TMS) oligonucleotides, which inhibit telomerase. PGEk (64 amino-acid residues) contains a hydrophobic domain that originates from the human epidermal growth factor (hEGF) and is responsible for the receptor-mediated transfer of PGEk across the cell membrane, and the hydrophilic domain, which is a nuclear localization signal (NLS) and serves to bind DNA and deliver it to the cell nucleus. Experiments were performed in 0.01-M Na-phosphate and 0.1-M NaCl at 37°C. An analysis of the circular dichroism (CD) spectra showed that TMO forms an antiparallel G-quadruplex, while TMS occurs in the form of unfolded strands. The number of PGEk molecules adsorbed on oligonucleotides was estimated from the quenching of PGEk fluorescence and the increase in its polarization upon titration with oligonucleotides. Adsorption isotherms were plotted in Scatchard coordinates. Adsorption of the first two PGEk molecules on TMO and TMS followed a noncooperative mechanism and was characterized by high association constants: $K_{1(TMO)} = (7 \pm 1) \cdot 10^7$ M^{-1} and $K_{1(TMS)} = (3 \pm 0.5) \cdot 10^7$ M^{-1}. Further adsorption, up to five or six PGEk molecules per TMO molecule, showed high cooperation and $K_{2(TMO)} = (4.0 \pm 1.5) \cdot 10^6$ M^{-1}. Unlike TMO, TMS only weakly bound the third PGEk molecule: $K_{2(TMS)} = (8 \pm 2) \cdot 10^5$ M^{-1}. An analysis of the CD spectra showed that PGEk partly unfolded the G-quadruplex formed by TMO and did not have an effect on the single-stranded structure of TMS. The secondary structure of DNA and the number of protein subunits were established for the biologically active complexes PGEk–TMO and PGEk–TMS, which efficiently pass across the membrane of cancer cells and inhibit their proliferation.

DOI: 10.1134/S0026893306030101

Key words: DNA G-quadruplex, protein carrier, proliferating cells, telomerase inhibitors, spectral methods

INTRODUCTION

DNA sequences enriched in guanine repeats (G)$_n$ are capable of forming stable four-stranded structures known as G-quadruplexes. The G-quadruplex structure is stabilized by hydrogen bonding within the G quartets and stacking contacts between the quartets [1]. Recent studies have demonstrated that G quadruplexes exist in the cell nucleus [2, 3], and play a role in regulating gene expression [4]. In the human genome, G-rich DNA sequences have been found in centromeres, the repeats belonging to the fragile-X gene [5], some gene promoters [1], and in the telomeres at the ends of linear chromosomes [6].

The structure of telomeric DNA has received much attention in the past few years. Telomeres ensure the completion of chromosomal DNA replication and protect the chromosome ends from sticking and degradation [7–11]. Human G-rich telomeric DNA contains d(TTAGGG)$_n$ repeats and ends with a single-stranded 3'-overhang [7, 8]. The 3'overhang is involved in regulating the telomerase activity and the telomere–telomere interactions [7, 12, 13]. The telomeres grow shorter after each cell division, and cells stop proliferating when a critical telomere size is achieved [14, 15]. Cancer cells are capable of unlimited proliferation owing to reactivation of telomerase, the enzyme that regulates the telomere length [7, 8, 10, 16–18].

Experiments in vitro have shown that the d(TTAGGG)$_4$ G-quadruplex inhibits telomerase [19–24]. Hence, it is important to find an effective means to deliver telomeric d(TTAGGG)$_4$ oligonucleotides, as telomerase inhibitors, into the nuclei of cancer cells.

Special methods have been developed to deliver oligonucleotides into cells. A promising way is to design protein and peptide vectors that carry genetic material into the cell [25–32], in particular, using fragments of viral envelope proteins [27]. It should be noted, however, that the effect of viral protein fragments on the human organism is still unknown. We think it is more advantageous to construct vectors with a high affinity for target cells on the basis of natural human proteins or their close homologs.

In this work we used the new recombinant protein vector PGEk (64 amino acid residues) [31] to deliver the telomeric oligonucleotide $d(TTAGGG)_4$ into the nuclei of cancer cells. PGEk selectively enters cancer cells via receptor-mediated endocytosis and is selective in respect to the cell nucleus and specific for nucleic acids. The human epidermal growth factor (hEGF) was used as a receptor-binding domain. Fragments of various growth factors have been employed successfully in the targeted delivery of cytostatics and the construction of vectors for gene therapy [32–35]. A DNA-binding domain is based on the human nuclear localization signal (NLS), consists of 11 amino acid residues (KKKKRKVEDPY), and is involved in DNA binding. PGEk efficiently transfers oligonucleotides and plasmid DNA into target cells [31]. Its complexes with phosphodiester (TMO) and phosphorothioate (TMS) derivatives of $d(TTAGGG)_4$ cause death to various cancer cells possessing EGF receptors [31].

In this work we studied the complexation of PGEk with TMO and TMS under near physiological conditions. PGEk proved to have a high affinity for telomeric G-quadruplexes formed by $d(TTAGGG)_4$ repeats. We determined the mechanisms, constants, and stochiometric parameters of PGEk binding.

The results can provide a basis for the construction of transport complexes with therapeutic oligonucleotides and PGEk.

EXPERIMENTAL

Reagents. Phosphodiester $d(TTAGGG)_4$ (TMO) and phosphorothioate $Sd(TTAGGG)_4$ (TMS) oligonucleotides were synthesized as in [28, 31, 35], isolated by reverse-phase ion-paired HPLC, and desalted.

Oligonucleotides were dissolved in PBS (10 mM Na-phosphate, pH 7.4, 0.1 M NaCl). The solutions were heated at 95°C for 5 min and quickly chilled to prevent intermolecular complexation [36, 37].

The oligonucleotide concentration was inferred from the UV spectra, using the molar extinction coefficient at 90°C ε_{260} = 11,000 M^{-1} cm^{-1} for $d(TTAGGG)_4$ and $Sd(TTAGGG)_4$ [38].

Recombinant PGEk was synthesized and purified as described in detail previously [31].

PGEk binding with oligonucleotides was carried out in PBS at 37°C.

To obtain the protein–nucleic acid complexes, a PGEk solution (1–2 μM) was combined with an oligonucleotide solution at the necessary molar ratio, and the mixture was incubated at 37°C for 5 min. The oligonucleotide concentration varied from 0.05 to 2 μM chains.

Instruments. The absorption spectra were recorded using a Jasco V-550 spectrophotometer. The fluorescence spectra and polarization were recorded using a Photon Technology instrument with a thermostatic cuvet unit. The circular dichroism (CD) spectra were recorded using a Jasco J715 dichrometer with a thermostatic cuvet.

UV fluorescence of PGEk was recorded in the range 310–460 nm, with excitation at 284 nm. Both the fluorescence intensity I and polarization P were measured at 340 nm.

Adsorption of PGEk on oligonucleotides. A PGEk solution in PBS with a constant concentration (1–2 μM) at 37°C was titrated with TMO and TMS, and the changes in I and P of PGEk fluorescence were recorded. The concentration of PGEk adsorbed on DNA was computed from the quenching of its own fluorescence as

$$\frac{C_2}{C_0} = \frac{(I_0 - I)}{(I_0 - I_2)}, \quad (1)$$

where I, I_0, and I_2 are, respectively, the PGEk fluorescence intensities measured in the presence and absence of oligonucleotides and for PGEk completely bound with oligonucleotides; $C_0 = C_1 + C_2$ is the total concentration of free (C_1) and bound (C_2) PGEk.

Polarization of PGEk fluorescence was obtained as

$$P = \frac{(I_\parallel - I_\perp)}{(I_\parallel + I_\perp)}, \quad (2)$$

where $I_\parallel$ and $I_\perp$ are the parallel and perpendicular components of fluorescence intensity upon excitation with vertically polarized light.

The concentration of bound PGEk was obtained from the equation

$$\frac{C_2}{C_0} = \frac{1}{\left[1 + \left(\frac{I_2}{I_0}\right)\frac{(P_2 - P)}{(P - P_0)}\right]}, \quad (3)$$

where P_0, P, and P_2 are, respectively, the fluorescence polarization measured in the absence and in the presence of oligonucleotides and for PGEk completely bound with oligonucleotides;

$$\frac{I_2}{I_0} = \frac{(I_{\parallel 2} + I_{\perp 2})}{(I_{\parallel 0} + I_{\perp 0})} \quad (4)$$

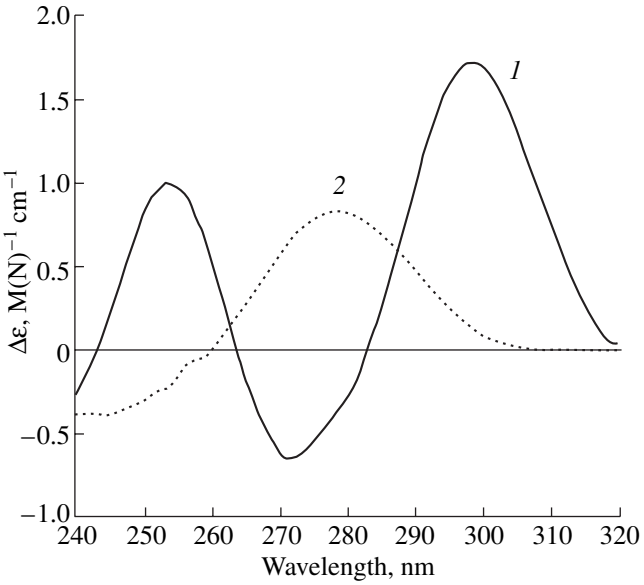

Fig. 1. CD spectra of (*1*) phosphodiester d(TTAGGG)$_4$ and (*2*) its phosphorothioate analog. Experiments were performed with 1 μM oligonucleotides in PBS at 37°C.

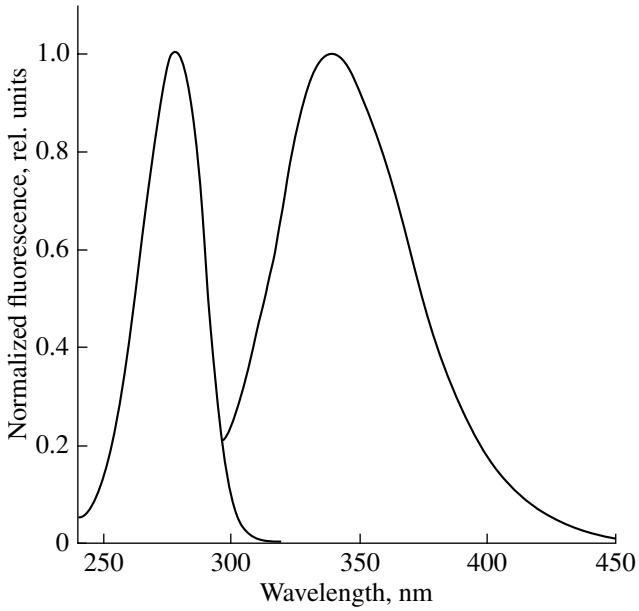

Fig. 2. Excitation and fluorescence spectra of the protein vector PGEk in PBS at 37°C. The excitation wavelength was 284 nm.

is the ratio of the polarized fluorescence intensities of the bound and free PGEk, respectively.

Isotherms of PGEk adsorption on TMO and TMS were plotted in Scatchard coordinates, as an r dependence of r/c_1. The parameter $r = C_2/C_{DNA}$ corresponds to bound PGEk per oligonucleotide.

In the case of a noncooperative mechanism of PGEk binding, we used the equation

$$K_a = \frac{C_2}{C_1(C_{DNA}N - C_2)}, \quad (5)$$

where K_a is the association constant; C_2 and C_1 are the concentrations of bound and free PGEk, respectively; C_{DNA} is the molar concentration of the oligonucleotide chains; and N is the maximal number of PGEk-binding sites on the oligonucleotide.

In the case of the cooperative mechanism of PGEk binding, we used the equation

$$K_a^{\omega} = \frac{C_2}{C_1^{\omega}(C_{DNA}N - C_2)}, \quad (6)$$

where K_a is the association constant and ω is the cooperative binding coefficient [39].

RESULTS AND DISCUSSION

Conformations of Phosphodiester and Phosphorothioate d(TTAGGG)$_4$ Oligonucleotides

To study the DNA complexation with PGEk, we used TMS and TMO, which suppressed the telomerase activity in vitro [19–24, 40–42] and the growth of actively proliferating cells [31]. The conformational properties of the oligonucleotides were inferred from their CD spectra. Figure 1 shows the CD spectra of TMO (curve *1*) and TMS (curve *2*). The TMO spectrum included a positive band with a maximum at about 295 nm and a negative band at about 260–270 nm, which corresponds to the CD spectrum of an antiparallel G-quadruplex [38, 43, 44]. The CD spectrum of TMS had a weak positive band with a maximum at about 278 nm, as characteristic of a denatured phosphorothioate DNA strand, which virtually completely lacks stacking contacts between the bases [45].

UV Fluorescence of the Protein Vector PGEk and Its Changes in Complex with TMO or TMS

The excitation and fluorescence spectra of PGEk are shown in Fig. 2. The shape and position of the excitation (λ = 284 nm) and fluorescence (λ = 340 nm) maximums correspond to the fluorescence of the Trp residues of PGEk [46, 47]. Figure 3 shows the changes in fluorescence intensity at 340 nm (a) polarization (b) in the presence of oligonucleotides. Fluorescence intensity decreased and polarization increased as the concentration of TMO or TMS increased. Both I and P reached their extreme values at the molar ratios TMO:PGEk = 0.5 and TMS:PGEk = 0.8. The changes in the polarization and intensity of UV fluorescence of PGEk reflected its sorption on oligonucleotides.

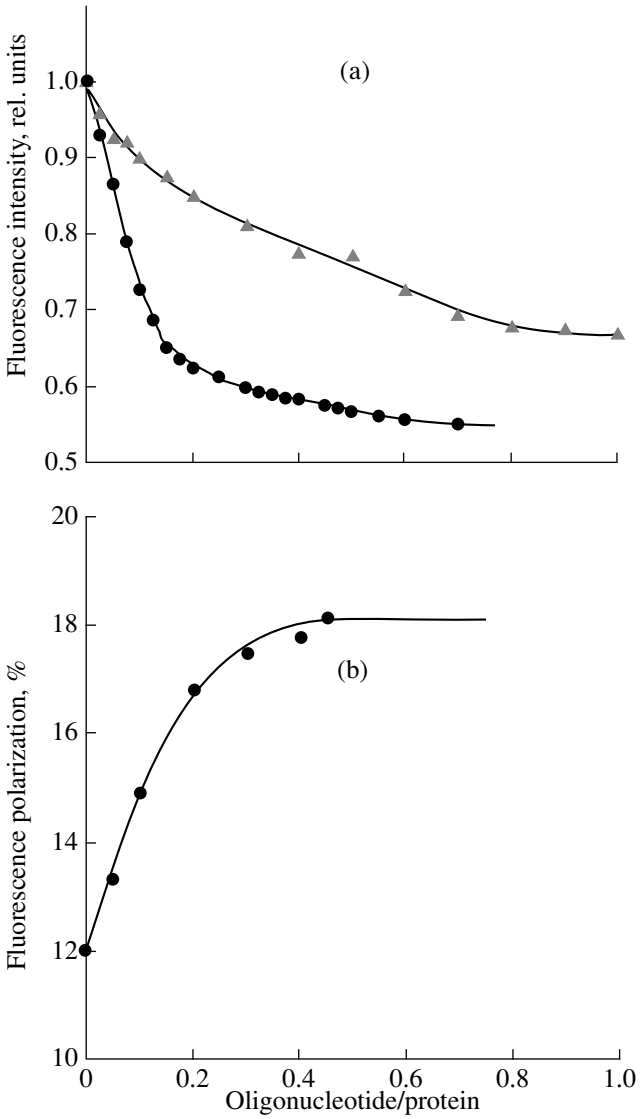

Fig. 3. Changes in (a) intensity and (b) polarization of PGEk fluorescence in the presence of TMO (circles) or TMS (triangles). Experiments were performed in PBS at 37°C; PGEk was used at 2 μM; the oligonucleotide concentration was varied from 0.05 to 2 μM.

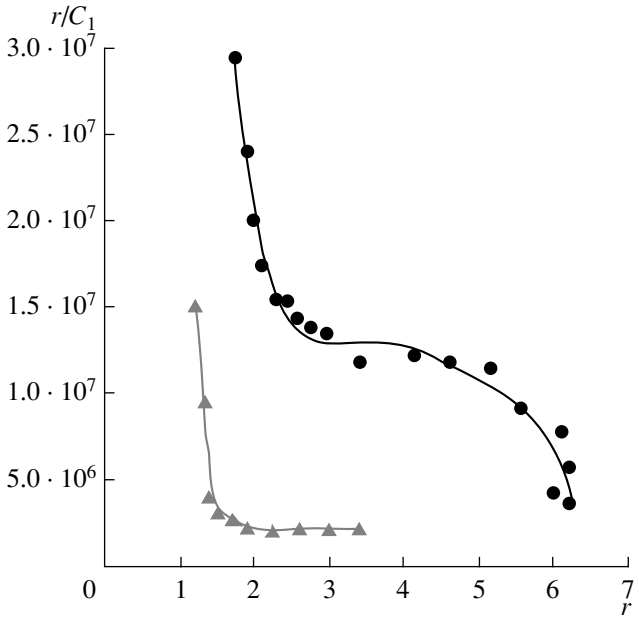

Fig. 4. Isotherms of PGEk adsorption on TMO (●) and TMS (▲) in the form of an r dependence of r/C_1, where r is the number of bound PGEk molecules per oligonucleotide and C_1 is the free protein concentration. Experiments were performed in PBS at 37°C.

Isotherms of PGEk Adsorption on TMO and TMS

The isotherms of PGEk adsorption on TMO and TMS were presented as an r dependence of r/C_1, where $r = C_2/C_{DNA}$ is the binding protein concentration divided by the oligonucleotide concentration (Fig. 4). To construct isotherms we used the data presented in Fig. 3 and Eqs. (1) and (3). It is seen that the adsorption of PGEk on TMO and TMS at the interval $r \le 2.0$ is well described by the noncooperative binding model (Eq. (5)).

The intersection with the abscissa reports the number of strong binding sites N_1. The tangent of the slope is numerically equal to the association constant: $K_{1(TMO)} = (7 \pm 1) \cdot 10^7$ M^{-1} and $K_{1(TMS)} = (3 \pm 0.5) \cdot 10^7$ M^{-1}. In the range $2.0 < r \le 6 \pm 0.3$, the binding of PGEk with TMO was clearly cooperative and was well described by Eq. (6) obtained for such cases: the association constant $K_{2(TMO)} = (4 \pm 1.5) \cdot 10^6$ M^{-1}, the cooperativeness coefficient $\omega = 3.4$, and the maximal number of binding sites $N = 6 \pm 0.3$. Unlike with TMO, adsorption of PGEk on TMS sharply decreased at $r \ge 2$. The association constant estimated for the third and subsequent PGEk molecules was $K_{2(TMS)} \le (8 \pm 2) \cdot 10^5$ M^{-1}, two orders of magnitude lower than $K_{1(TMS)}$. The difference in PGEk binding with TMO and TMS can be explained by the considerable difference in their secondary structures. An analysis of the CD spectra (Fig. 1) showed that TMO molecules fold into an antiparallel G-quadruplex, while TMS molecules lack a distinct secondary structure and occur as unfolded strands.

Upon the maximal binding of PGEk on TMO ($N = 6 \pm 0.3$), there are four phosphate groups for every PGEk molecule. The NLS domain of PGEk, which is responsible for DNA binding, consists of 11 amino acid residues, including six that are positively charged (KKKKRK-). The first four Lys residues probably directly contact DNA [31]. If so, one phosphate of the TMO molecule corresponds to one Lys of the PGEk molecule.

The flexible denatured TMS strand may readily adapt to the structure of the NLS domain (11 residues) and interact with all positively charged amino acid residues of NLS. The highest number of PGEk binding

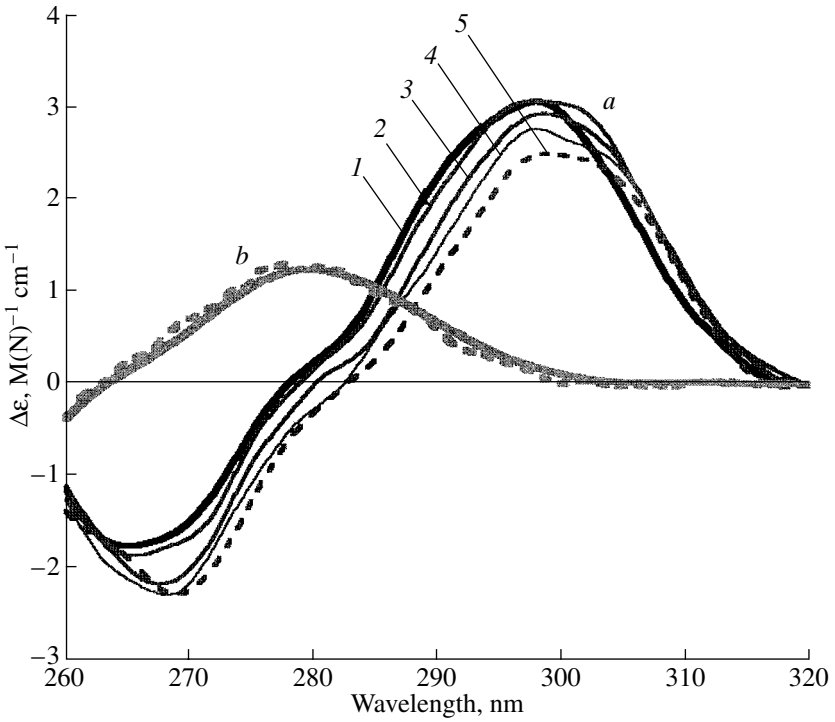

Fig. 5. (a) CD spectra of PGEk:TMO complexes. The initial concentration of TMO was 0.9 μM. The PGEk/TMO ratio was (*1*) 0, (*2*) 1.7, (*3*) 2.6, (*4*) 3.4, and (*5*) 5.1. (b) CD spectra of PGEk:TMS complexes. The initial concentration of TMS was 3.7 μM. The spectra were recorded in the absence of PGEk (solid line) and with PGEk used at two molecules per oligonucleotide (dashed line).

sites on the TMS molecule would not be more than $N = 3$, which agrees with the experimental data (Fig. 4).

The high association constants obtained for six PGEk molecules and TMO suggest that electrostatic interactions make the greatest contribution to the PGEk binding with DNA.

The constants and stoichiometry of the PGEk binding with TMO were compared with the corresponding binding parameters reported for the peptide vector MPG and a single-stranded 18-mer phosphodiester oligodeoxyribonucleotide [27]. MPG consists of 27 amino acid residues. Its hydrophobic domain originates from a fragment of the fusogenic protein gp41 of HIV-1. The C-terminal hydrophilic domain includes NLS of the SV40 T-antigen. The DNA-binding NLS domain of MPG contains four positively charged residues (-KKKR-). Energy migration between Trp of MPG and fluorescent manzyl covalently linked to an oligonucleotide has been used to estimate the maximal number of MPG molecules directly contacting a DNA fragment ($N = 4$) and their association constant $K = (8.5 \pm 1.3) \cdot 10^7\ M^{-1}$. With this stoichiometry one phosphate group of DNA corresponds to one positively charged amino acid residue, as in the case of PGEk:TMO. The association constant of MPG and DNA is of the same order of magnitude as the constants obtained for the two types of PGEk:TMO complexes: $(7 \pm 1) \cdot 10^7\ M^{-1} \geq K_{1,\,2(TMO)} \geq (4.0 \pm 1.5) \cdot 10^6\ M^{-1}$. The experiments with MPG were performed in 9.8 mM PBS at 25°C; i.e., the ionic strength and temperature were lower than in our experiments (10 mM PBS, 0.1 M NaCl, 37°C). Thus, there is a good agreement of the energy and stoichiometric parameters of the binding with phosphodiester DNA between PGEk and MPG, which again confirms our assumption that the energy of PGEk binding with phosphodiester telomeric DNA fragments depends mostly on the electrostatic interactions between the positively charged residues of the NLS domain and the negatively charged phosphate groups of the nucleic acid.

An analysis of the adsorption isotherms showed that six PGEk molecules have a high affinity for the G-quadruplex formed by telomeric $d(TTAGGG)_4$ repeats.

It should be noted that our estimates of the number of binding sites correlate with the effect of various excesses of PGEk on the biological activities of TMO and TMS. We have observed previously that, in the absence of PGEk, TMO and TMS used at 1–2 μM do not exert a cytotoxic effect on cancer cells, including MCF-7 [31]. An essentially different effect on cell viability has been obtained with oligomers delivered into cells in the form of PGEk:DNA complexes with the ratio 5:1 [31]. The results of more detailed studies with several cell lines will be reported in forthcoming articles.

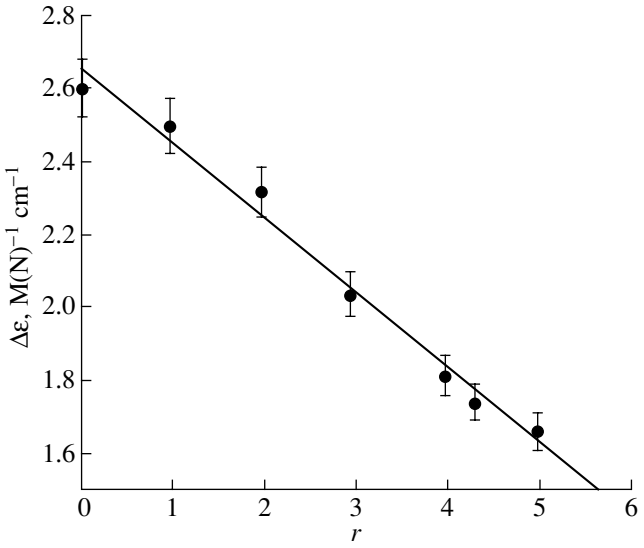

Fig. 6. Changes in the amplitude of the CD spectrum of TMO at 290 nm, with increasing number of adsorbed PGEk molecules per oligonucleotide (*r*).

Effect of PGEk Molecules on the Structure of a G-Quadruplex Formed by d(TTAGGG)$_4$ Repeats

We used CD spectra to detect the structural changes occurring in the G-quadruplex of d(TTAGGG)$_4$ repeats in response to PGEk adsorption. The CD spectrum of the G-quadruplex in the region 260–320 nm changed with increasing PGEk concentration in the solution: the amplitude became considerably lower at 290–295 nm and the maximum was shifted to 300 nm (Fig. 5). Protein molecules do not have an appreciable optical activity in this spectral region and do not contribute to the CD spectra of the G-quadruplex. The decrease in amplitude at about 290 nm depended linearly on the number of adsorbed protein molecules *r* (Fig. 6), suggesting that the adsorption of each PGEk molecule on the G-quadruplex slightly changes its conformation, e.g., partly unwinds the four-stranded helix.

The CD spectra of TMS displayed only minor, if any, changes upon the adsorption of PGEk molecules (Fig. 5). It is possible to assume on this evidence that TMS molecules retain their single-stranded state in complex with PGEk.

To summarize, we established the mechanisms of adsorption, the constants, and the stoichiometry of binding for PGEk interacting with TMO and TMS. PGEk proved to have a high affinity for the G-quadruplex formed by phosphodiester TMO. In complex with PGEk, TMO occurs as a G-quadruplex structure, while TMS remains unfolded. The structural organization was determined for the biologically active PGEk:DNA complexes.

ACKNOWLEDGMENTS

This work was supported by the Russian Foundation for Basic Research (project nos. 02-04-49182, 04-04-49618), the Russian Foundation for Basic Research–MAS (project no. 03-04-06825), and an FEBS Fellowship 2005.

REFERENCES

1. Simonsson T. 2001. G-quadruplex DNA structure: Variations on a theme. *Biol. Chem*. **382**, 621–628.
2. Schaffitzel C., Berger I., Postberg J., Hanes J., Zipps H.J., Pruckthan A. 2001. In vivo generated antibodies specific for telomeric guanine—quadruplex DNA react with *Stylonychia lemnae* macronuclei. *Proc. Natl. Acad. Sci. USA*. **98**, 8572–8577.
3. Paeschke K., Simonsson T., Postberg J., Rhodes D., Lipps H.J. 2005. Telomere end binding protein control the formation of G-quadruplex DNA structures in vivo. *Nature Struct. Mol. Biol*. **12**, 847–854.
4. Siddiqui-Jain A., Grand C.L., Bearss D.J., Harley L.H. 2002. Direct evidence for a G-quadruplex in a promoter region and its targeting with a small molecule to repress *cMyc* transcription. *Proc. Natl. Acad. Sci. USA*. **99**, 11593–11598.
5. Usdin K. 1998. NGG-triplet repeats form similar intrastrand structures: Implications for the triplet expansion diseases. *Nucleic Acids Res*. **26**, 1167–1172.
6. Wright W.E., Tesmer W.M., Huffman K.E., Levene S.D., Shay J.W. 1997. Normal human chromosomes have long G-rich telomeric overhangs at one end. *Genes Dev*. **11**, 2801–2809.
7. Blackburn E.H. 1991. Structure and function of telomeres. *Nature*. **350**, 569–573
8. Blackburn E.H. 1992. Telomerases. *Annu. Rev. Biochem*. **61**, 113–129.
9. Mc Eachern M.J., Krauskopf A., Blackburn E.H. 2000. Telomeres and their control. *Annu. Rev. Genet*. **34**, 331–358.
10. Blackburn E.H. 2001. Switching and signaling at the telomere. *Cell*. **106**, 661–673.
11. Zakian V.A. 1995. Telomeres beginning to understand the end. *Science*. **270**, 1601–1607.
12. Makarov V.L., Hirose Y., Langmore J.P. 1997. Long G-tails at both ends of human chromosomes suggest a C-strand degradation mechanism for telomere shortening. *Cell*. **88**, 657–666.
13. Wright W.E., Tesmer V.M., Huffman K.E., Zavene S.D., Shay J.W. 1997. Normal human chromosomes have a long a rich telomeric overhangs at one end. *Genes Dev*. **11**, 2801–2809.
14. De Lange T. 2002. Protection of mammalian telomeres. *Oncogene*. **21**, 532–540.
15. Harley C.B., Futcher A.B., Greider C.W. 1990. Telomeres shorten during ageing of human fibroblasts. *Nature*. **345**, 458–460.
16. Greider C.W. 1998. Telomerase activity, cell proliferation, and cancer. *Proc. Natl. Acad. Sci. USA*. **95**, 90–92.

17. Han H., Harley L.H. 2000. G-quadruplex DNA: A potential target for anti-cancer drug design. *TIPS*. **21**, 136–141.

18. Kim N.W., Piatyszek M.A., Prowse K.R., Harley C.B., West M.D., Ho P.L.C., Coviello G.H., Wright W.E., Weinrich S.L., Shay J.W. 1994. Specific association of human telomerase activity with immortal cells and cancer. *Science*. **266**, 2011–2015.

19. Simonsson T. 2001. G-quadruplex DNA structure: Variations on a theme. *Biol. Chem*. **382**, 621–628.

20. Williamson J.R. 1994. G-quartet structures in telomeric DNA. *Annu. Rev. Biophys. Biomol. Struct*. **23**, 703–730.

21. Neidle S., Read M.A. 2001. G-quadruplex as therapeutic targets. *Biopolymers*. **56**, 195–208.

22. Zahler A.M., Williamson J.R., Cech T.R., Prescott D.M. 1991. Inhibition of telomerase by G-quartet structures. *Nature*. **350**, 718–720.

23. Sun D., et al. 1997. Inhibition of human telomerases by G-quadruplex-interactive compound. *J. Med. Chem*. **40**, 2113–2116.

24. Neidle S., Parkinson G.N. 2003. The structure of telomeric DNA. *Curr. Opin. Struct. Biol*. **13**, 275–283.

25. Shiraishi T., Hamzavi R., Nielsen P.E. 2005. Targeting delivery of plasmid DNA into the nucleus of cell via nuclear localization signal peptide conjugate to DNA Intercalating bis- and trisacridines. *Bioconjugate Chem*. **16**, 1112–1116.

26. Felgner P.L., et al. 1987. Lipofection: A highly efficient lipid-mediated DNA transfection procedure. *Proc. Natl. Acad. Sci. USA*. **84**, 7413–7417.

27. Morris M.C., Vidal P., Chaloin L., Heitz F., Divita G. 1997. A new peptide vector for efficient delivery of oligonucleotides into mammalian cells. *Nucleic Acids Res*. **25**, 2730–2736.

28. Pozmogova G.E., Chuvilin A.N., Posypanova G.N., Shulga A.A., Ermolyuk Yu.S., Kireeva N.N., Kirpichnikov M.P., Skryabin K.S. 2001. New EGF—based peptide vectors for antisence oligonucleotides and plasmid DNA target delivery into actively proliferating cells. *Proc. Int. Conf. RNA As Therapeutics and Genomics Target*. Novosibirsk, p. 83.

29. Richardson P.D., Crein B.T., Steer C.J. 2002. Gene repair in the new age of gene therapy. *Hepatology.* **35**, 512–518.

30. Zubin E.M., Romaniva E.A., Orteskaya T.S. 2002. Modern methods of oligonucleotidepeptide synthesis. *Usp. Khim*. **71**, 273–301.

31. Pozmogova G.E., Chuvilin A.N., Posypanova G.A., Shulga A.A., Eldarov M.A., Ermolyuk Ya.S., Severin E.S., Kirpichnikov M.P., Skryabin K.G. 2004. RF Patent no. 2248983.

32. Sosnowski B.A., Gonzalez A.N., Buechler Y.J., Pierse G.F., Baird A. 1996. Targeting DNA to cells with basic fibroblast growth factor (FGF2). *J. Biol. Chem*. **271**, 33647–33653.

33. Wels W., Moritz D., Schmidt M., Jeschke H., Hynes N.E., Groner B. 1995. Biotechnological and gene therapeutical strategies in cancer treatment. *Gene*. **159**, 73–80.

34. Cristiano R.J., Roth J.A. 1996. Epidermal growth factor mediated DNA delivery into lung cancer cells via the epidermal growth factor receptor. *Cancer Gene Ther.* **3**, 4–10.

35. Frederiksen K.S., Abrahamsen N., Cristiano R.J., Damstrup L., Poulsen H.S. 2000. Gene delivery by an epidermal growth factor/DNA polyplex to small cell lung cancer cell lines expressing low levels of epidermal growth factor receptor. *Cancer Gene Ther.* **7**, 262–268.

36. Shchyolkina A.K., Borisova O.F., Livshits M.A., Pozmogova G.E., Chernov B.K., Klement R., Jovin T.M. 2000. Parallel-stranded DNA with mixed AT/GC composition: Role of trans-GC base pairs in sequence dependent helical stability. *Biochemistry.* **39**, 10034–10044.

37. Besschetnova I.A., Pozmogova G.E., Shchyolkina A.K., Borisova O.F. 2005. The effect of the secondary and tertiary structure of $d(TTAGGG)_4$ telomeric oligonucleotides on their binding with novel recombinant protein PGEk: Deliver of DNA in cell. *J. Biomol. Struct. Dynam*. **22**, 859–860.

38. Balagurumoorthy P., Brahmachari S.K. 1994. Structure and stability of human telomeric sequence. *J. Biol. Chem*. **269**, 12858–12869.

39. Cantor C.R., Schimmel P.R. 1980. *Biophysical Chemistry.* San Francisco: W.H. Freeman.

40. Glukhov A.I., Zimnik O.V., Gordeev S.A., Severin S.E. 1998. Inhibition of telomerase activity of melanoma cells in vitro by antisence oligonucleotides. *Biochem. Biophys. Res. Commun*. **248**, 368–371.

41. Herbert B., Pitts A.E., Baker S.I., Hamilton S.E., Wright W.E., Shay J.W., Corey D.E. 1999. Inhibition of human telomerase in immortal human cells leads to progressive telomere shortening and cell death. *Proc. Natl. Acad. Sci. USA*. **96**, 14276–14281.

42. Harley C.B. 2002. Telomerase is not an oncogene. *Oncogene*. **21**, 494–502.

43. Balagurumoorthy P., Brahmachari S., Mohanty D., Bansal M., Sasisekharan V. 1992. Hairpin and parallel quartet structures for telomeric sequences. *Nucleic Acids Res*. **20**, 4061–4067.

44. Miyoshi D., Nakao A., Toda T., Sugimoto N. 2001. Effect of divalent cations on antiparallel G-quartet structure of d(G4T4G4). *FEBS Lett*. **496**, 128–131.

45. Clark Ch.L., Cecil P.K., Singh D., Gray D.M. 1997. CD, adsorption and thermodynamic analysis of repeating dinucleotide DNA, RNA and hybrid duplexes $[d/r(AC)_{12}[d/r(GT/U)]_{12}$ and the influence of phophorothioate substitution. *Nucleic Acid Res*. **25**, 4098–4105.

46. Burstein E.A., Vedenkina N.S., Ivkova M.N. 1974. Fluorescence and the localization of tryptophan residues in protein molecules. *Photochem. Photobiol*. **18**, 263–279.

47. Chen Y., Barkley M.D. 1998. Toward understanding tryptophan fluorescence in proteins. *Biochemistry.* **37**, 9976–9982.